Journal of Engineering Physics and Thermophysics, Vol. 83, No. 4, 2010

IDENTIFICATION OF MODELS AND PREDICTION OF PHYSICAL PROPERTIES OF HIGHLY POROUS HEAT-SHIELDING MATERIALS

O. M. Alifanov and V. V. Cherepanov

UDC 519.6:535.2:536.3

A complex procedure has been proposed, which allows determining and predicting a significant part of the physical properties of heat-shielding highly porous materials. It is based on the combination of experiment, statistical methods of mathematical modeling, methods of solving the problem of radiation transfer, and methods of identifying mathematical models in solving pertinent inverse problems. Apart from decreasing expenditures, this approach markedly expands the capabilities of experimental methods. It allows studying and predicting components of the thermal conductivity, energy accommodation coefficient, complex refractive index and dielectric constant, scattering indicatrix, etc. As an element of the proposed approach, an original method of numerical solution of radiation transfer in a heterogeneous plane layer has been described. The results can be used for developing new materials and nondestructive methods of control and diagnostics, designing thermal-protection systems, etc.

Keywords: *highly porous materials, thermal experiments, methodology, thermal physical properties, determination and prediction, radiation transfer, integral equation, functional minimization, conjugate-gradient method, stabilization.*

Introduction. The principal trends in the development of many state-of-the-art technical systems involve an increase in the number of thermally loaded elements in them, as well as more stringent operating conditions and requirements for reliability and guaranteed service life, and a reduction in the specific metal content. Such features of modern problems of thermal design as nonstationarity, nonlinearity, multidimensionality of the heat load, and account for the combined nature of heat and mass transfer limit the possibility of using many traditional designing methods and necessitate the development of new materials and structures. Specifically, this applies to space and aerospace vehicles for which the provision of required thermal operating conditions is among the most important problems in designing. The production of heat-shielding and heat-insulating materials with preset properties plays here the key role. Regrettably, a direct measurement of many important physical characteristics is practically unfeasible. Therefore it is impossible to develop new promising materials with preset properties without extensive use of the methods of mathematical modeling. Their application markedly expands experimental potentials and significantly reduces expenditures at the step of designing. In turn, mathematical modeling is impossible without reliable information on specific features and properties of the materials and systems, which can be given only by physical experiment. Therefore, combining the methods of mathematical modeling of the structure of the material and heat and mass transfer in it with the results of indirect measurements, in which the needed properties of the system are analyzed through direct measurements of relatively accessible quantities (such as temperatures, mass fractions and densities, indices of anisotropy, etc.), and the solution of pertinent problems of identifying, for example, inverse problems of heat transfer [1], make it possible to solve the problems enumerated above. A general idea of this approach is illustrated by the scheme in Fig. 1. In this connection, some explanations will be given.

The methods of inverse problems of heat transfer were developed for increasing informativeness of thermal experiments and tests and improving accuracy and reliability of the processing and identification of experimental data. In most cases, this methodology is used as the most rational, and in many practical situations, also as the only accessible one (e.g., in determining thermal properties of materials with the memory of heating or cooling conditions). The

Moscow Aviation Institute (State Technical University), 4 Volokolamskoe Highway, Moscow, 125993, Russia; email: bold@tushino.com. Translated from Inzhenerno-Fizicheskii Zhurnal, Vol. 83, No. 4, pp. 720–732, July–August, 2010. Original article submitted March 2, 2010.

 1062-0125/10/8304-0770

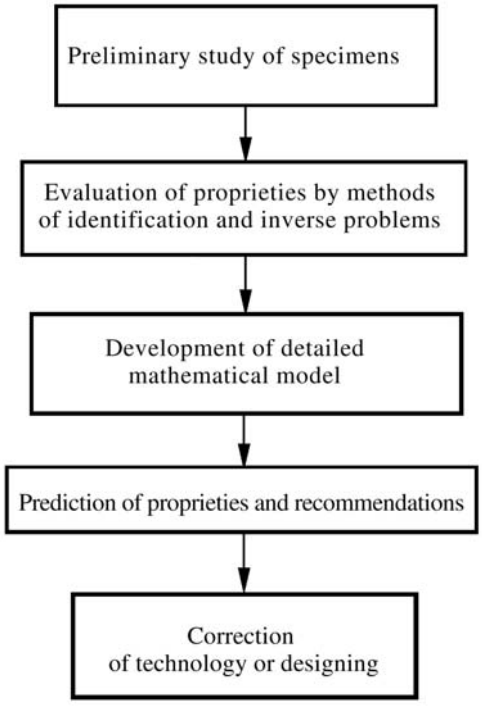

Fig. 1. Analysis and prediction of properties.

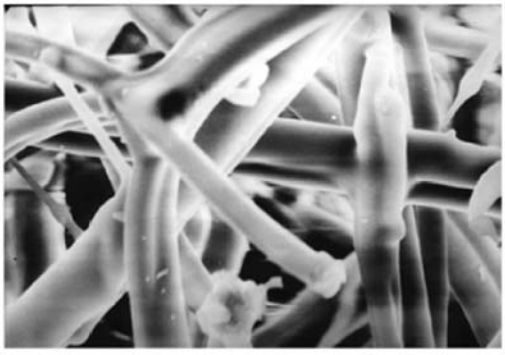

Fig. 2. Structure of an Li-900 FM material.

disturbance of cause and effect relationships in the formulation of these problems renders them mathematically ill-posed (it most frequently leads to the absence of a unique or stable solution). In order to solve such problems we develop special methods based on the mathematical theory of ill-posed problems and generally called regularization. Successful use of the methodology of inverse problems necessitates a skillful combination of physical modeling of heat transfer in specimens and sufficiently accurate measurements of thermal parameters, as well as correct mathematical processing of experimental data [2].

Lightweight highly porous heat-shielding materials, such as fibrous materials, foam materials with accessible porosity, etc., are of great interest for many aerospace and other applications. They either consist of randomly oriented fibers or have a mesh space skeleton formed by irregular shaped nodes and bridges (Fig. 2).

On the one hand, experimental study of the material is possible only after its specimens have been actually produced. On the other hand, interpreting the experimental results aimed at determining various components of physical parameters of the material is in many cases fairly complicated. Considerable problems also arise in determining parameters of the material if their values are governed by processes of purely local or spectral character. Moreover, the very possibility of determining and predicting such properties of the material is substantially limited or they even cannot be determined without resorting to the tools of mathematical modeling. Among these properties are such quantities

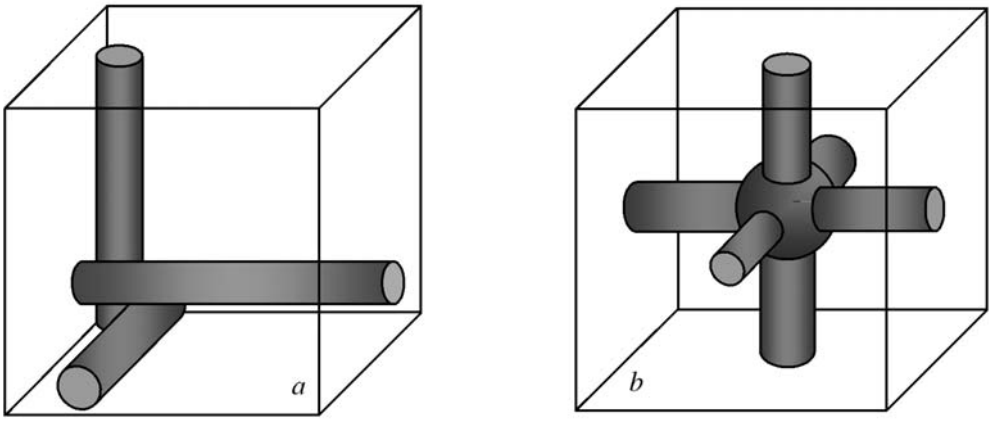

Fig. 3. Representative elements of models: a) of fibrous materials and b) of foam materials.

as the complex refractive index and dielectric constant, coefficients of radiation scattering and absorption, scattering indicatrix, etc.

Mathematical Modeling of Materials. Global irregularity, heterogeneity, and anisotropy of highly porous materials appreciably narrow the range of approaches to mathematical modeling of their structure and properties. Still, such systems are locally regular [3, 4]. This allows one to isolate regular representative elements in the system (Fig. 3), describe their properties, and on this basis carry out calculations in regard to both individual aspects of the problem and properties of the material as a whole.

It should be noted that in modeling the material as a whole it is possible to formulate and calculate the entire complex of its determining properties. Here it should be pointed out that there is still no alternative to the approach to modeling the materials of VALOX, KR, TZMK, TZM, ETTI, RVC, and other types, which uses modeling of an actually irregular structure based on a stochastic regular and orthogonal model system consisting of spheres and cylindrical fibers [4, 5]. A more detailed description of the generation of representative elements and of the determination of their characteristics is given in [5]. Here we note only some points of this process.

Representative elements of the model structure have several key parameters largely determining the thermal physical properties of the model system. Alongside the material properties, the determining parameters for the considered materials are the indices of anisotropy $a_{1,2}$ in the directions orthogonal to heat transfer. Their values are determined either as a ratio of thermal conductivities measured along the principal axes or by the method of mechanical loads. We prefer the first method, since the most important property of the material from the standpoint of thermal designing is its thermal conductivity. For fibrous materials, among the key parameters is also the dimension of a representative element in the direction of heat transfer, and in the case of foam materials, to the key parameters belong the coefficient of cutting off of bridges, which determines the portion of the bridge part included in a representative element. Their "reference" value is governed by the condition that the mass density of the system of representative elements should be the same as the density of the considered porous material. The corresponding equations for these quantities denoted for brevity by x are of the form

$$\sum_{k=1}^{N_\mathrm{b}} P_{\mathrm{b},k} \sum_{n_1=1}^{N_\mathrm{d}} P_{n_1} \sum_{m_1=1}^{N_\mathrm{len}} \frac{P_{n_1,m_1}}{0.5d_{\mathrm{b},k} + a_1 x l_{n_1,m_1}} \sum_{n_2=1}^{N_\mathrm{d}} P_{n_2} \sum_{m_2=1}^{N_\mathrm{len}} \frac{P_{n_2,m_2}}{0.5d_{\mathrm{b},k} + a_2 x l_{n_2,m_2}}$$

$$\times \sum_{n_3=1}^{N_\mathrm{d}} P_{n_3} \sum_{m_3=1}^{N_\mathrm{len}} \frac{P_{n_3,m_3}}{0.5d_{\mathrm{b},k} + x l_{n_3,m_3}} \left[\frac{d_{\mathrm{b},k}^3}{3} + x \left(d_{n_1}^2 l_{n_1,m_1} a_1 + d_{n_2}^2 l_{n_2,m_2} a_2 + d_{n_3}^2 l_{n_3,m_3} \right) \right] - \frac{16}{\pi} \frac{\rho}{\rho_0} = 0$$

for foam materials and

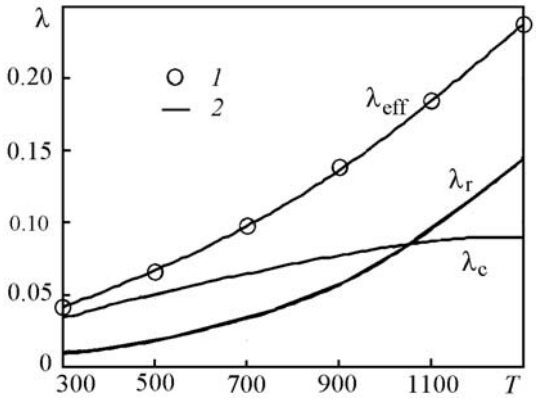

Fig. 4. Calculated results and experimental data for TZMK-10: λ_{eff}, total, λ_r, radiative, and λ_c, conductive thermal conductivity; 1) theory; 2) experiment. λ, W/(m·K); T, K.

$$\frac{1}{\langle d\rangle^2}\left\{a_1a_2\rho x^2-\frac{\pi}{12}\left(x\sum_{n=1}^{N_t}P_n\sum_{m=1}^{N_d}P_{n,m}\sum_{k=1}^{N_{len}}P_{n,m,k}\right)^{-1}\sum_{n=1}^{N_t}P_n\rho_n\sum_{m=1}^{N_d}P_{n,m}\left(d_{n,m+1}^2\right.\right.$$

$$\left.\left.+d_{n,m+1}d_{n,m}+d_{n,m}^2\right)\sum_{k=1}^{N_{len}}\frac{P_{n,m,k}}{l_{n,m,k+1}-l_{n,m,k}}\sum_{k=1}^{3}\int_{l_{n,m,k}}^{l_{n,m,k+1}}\left(\left[\frac{l}{a_kx}\right]+1\right)^{-1}ldl\right\}=0$$

for fibrous materials. The quantities entering into these relations form a statistical distribution of the base elements with respect to materials (types), diameters, and lengths. They are governed by the typical structure of data on the porous material, which should be available before the study of its properties is undertaken.

The thermal physical properties of the model system are very sensitive to the selection of the value of x. Its slight variation has a fairly strong effect on the density of the model system compared to the desired value. At the same time, the correct selection of the value of x does not yet guarantee obtaining satisfactory modeling results, since the quantities that characterize elements of the generated series are still chosen randomly. For example, in the case of fibrous materials with a marked spread of the same-type fibers in diameters, in two consequently generated series of representative elements it is practically impossible to obtain identical average values of thermal physical characteristics using the same value of x. Therefore, the generation process admits relatively small (generally within the limits of a 10% "corridor") variations in the values of x. Here the average density of the system of generated representative elements is collected such that it approaches the density of the modeled material. A variation in the element volume is appropriately allowed for in the value of its statistical weight.

In practical calculations, the generation of statistical elements ceases when the most important characteristics of the model system do not noticeably change any more. Among such characteristics is the average mass density. For materials with an insignificant spread in the characteristics of elements of this quantity it is quite sufficient to determine the condition of cessation of the generations. An increasing spread of elements, primarily in diameters, may be indicative of a noticeable difference in thermal physical characteristics of the systems with practically the same mass densities. In this event, in the criterion of cessation of the generation of representative elements the condition of density stabilization is completed with the condition of stabilization of the overall thermal conductivity, etc.

Since the position of a volume element in the material can be arbitrary, its elements are assumed to be surrounded by a medium whose thermal conductivity differs from the molecular thermal conductivity of clean gas by a correction for porosity. Such correction is given, for example, by the relation [3]

$$\lambda_p(T,\bar{p})=\frac{\lambda_{g0}(T)}{1+a(\bar{p}b)^{-1}},\quad \bar{p}=\frac{p}{p_0},\quad a=\frac{4\tilde{\gamma}(T)}{1+\tilde{\gamma}(T)}\frac{2-A(T)}{A(T)}\Lambda_0(T)\,\mathrm{Pr}^{-1}.$$

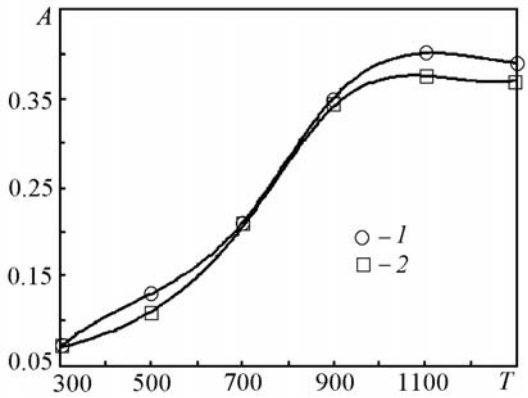

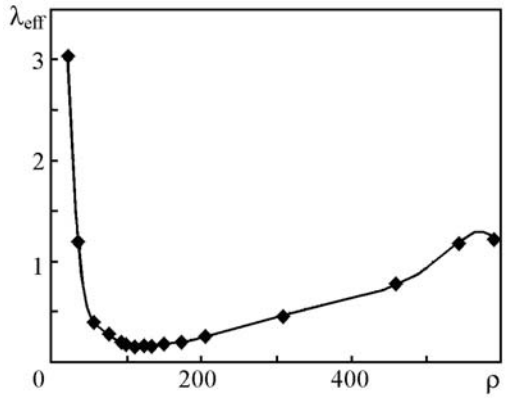

Fig. 5. Dependence $A(T)$ for TZMK-10 obtained from experimental results: 1) Moscow Aviation Institute and 2) All-Russian Institute of Aviation Materials. T, K.

Fig. 6. Total thermal conductivity as a function of mass density for ETTI-CF at t = 800°C (prediction). λ_{eff}, W/(m·K); ρ, kg/m^3.

If the assumption of local radiation equilibrium is justifiable, then, the radiative thermal conductivity λ_r can be calculated in a diffusional approximation [6], which leads to the relation (in the SI system of units)

$$\lambda_r(T) = 10^{-8}T^2\left(1.16\int_0^{10}\gamma^{-1}(\tau)\frac{\tau^4\exp(-\tau)}{(1-\exp(-\tau))^3}d\tau + 0.71T\int_0^{0.1}\gamma^{-1}(\tau)\frac{\tau^{-6}\exp(-\tau^{-1})}{(1-\exp(-\tau^{-1}))^3}d\tau\right).$$

The spectral coefficients of radiation scattering and attenuation β and γ are calculated using the Mie theory of spectral absorption [5, 7, 8].

Figures 4 and 5 present some results for the TZMK-10 fibrous material employed in elements of the thermal-protection system of the Buran space shuttle.

The available specimens of the material (manufactured by FGUP ONPP "Tekhnologiya") had density ρ = 144 kg/m^3. This material was made of fibers of high-purity melted quartz with ρ_1 = 2180 kg/m^3. Data on optical and thermal physical properties of amorphous quartz needed for calculations were borrowed from [9]. Figure 4 gives calculated curves of the temperature dependences for the total thermal conductivity λ_{eff}, as well as for its radiative λ_r and conductive λ_c components at normal pressure. The dependence $A(T)$ of the effective energy accommodation coefficient was selected using the experimental $\lambda_{eff}(T)$ curve for normal atmospheric pressure. The functions $A(T)$, which were determined in processing the data of the Moscow Aviation Institute and the All-Russian Institute of Aviation Materials, are presented in Fig. 5.

A similar statistical model was worked out for foam materials. As an example of its application, Fig. 6 shows the predicted dependence of the total thermal conductivity of the ETTI-CF-type foam vitreous carbon material on its density. ETTI materials were submitted for tests by the ASTRIUM GmBH corporation in association with ESTEC/ESA [2]. They were to be used for thermal insulation of structural elements of space vehicles within the framework of the project of flight to the Mercury "BepiColombo" carried out with the European Space Agency (ESA) and the Space Agency of Japan. The calculations indicated that, while not optimal in terms of thermal conductivity, the ETTI-CF material is nearly optimal in regard to the criterion $\lambda_{eff}\rho$, which makes it quite justifiable for use for the purposes stated above.

Modeling of Radiation Transfer in a Heterogeneous Layer. Method of Functional Optimization. If the assumption of local radiation equilibrium is not valid, radiative thermal conductivity of the material is determined within the framework of a kinetic approach. Central to this case is solving the equation of radiation transfer. We now elaborate on this issue.

Consideration is given to radiation transfer in a plane heterogeneous layer of the medium, such as a composite or porous material. This problem is spectral, since optical properties of the medium can exhibit spectral dependence.

We assume the temperature field in the layer and at its boundaries, and local spectral optical coefficients of the medium, to be stationary, preset, and independent of the amount of radiation. Suppose that radiation absorbed by the material is emitted in an equilibrium manner and the conditions of thermal equilibrium are maintained at the layer boundaries. Presumably, all properties of the medium and radiation can only change in the direction of the *Oz* axis oriented across the layer in the direction of heat transfer.

For many materials, in which heterogeneity and anisotropy are of random rather than regular character, it is permissible [5, 8] to use indicatrices dependent only on the cosine $\mathbf{\Omega}\cdot\mathbf{\Omega}_1 = \mu\mu_1 + \sqrt{1-\mu^2}\sqrt{1-\mu_1^2}\cos(\varphi-\varphi_1)$, $\mu = \cos\vartheta$, $\mu_1 = \cos\vartheta_1$ of the scattering angle, which are averaged over azimuths of the directions of incident and scattering radiation. Here the radiation intensity can be regarded as independent of the azimuth $u = u(z, \mu)$. As a result, we arrive at the known problem [10]

$$\left(\mu\frac{\partial}{\partial z}+\gamma(z)\right)u(z,\mu)=\alpha(z)\,u_{\mathrm{bl}}(z)+\beta(z)\int_{-1}^{1}\sigma(z,\mu,\mu_1)\,u(z,\mu_1)\,d\mu_1\,, \tag{1}$$

$$u(0,\mu)=u_{\mathrm{bl}}(0)\,,\quad \mu>0\,, \tag{2}$$

$$u(d,\mu)=u_{\mathrm{bl}}(d)\,,\quad \mu<0\,. \tag{3}$$

If the right-hand side of Eq. (1) is considered to be a known function, this equation can be solved by the method of variation of an arbitrary function, and integral equations of radiation transfer can be obtained [10, 11]:

$$u(z,\mu)=u_{\mathrm{bl}}(0)\exp\left[-\mu^{-1}\int_0^z\gamma(\tau)\,d\tau\right]$$

$$+\mu^{-1}\int_0^z\left[\alpha(\eta)\,u_{\mathrm{bl}}(\eta)+\beta(\eta)\int_{-1}^{0}\sigma(\eta,\mu,\mu_1)\,u(\eta,\mu_1)\,d\mu_1\right]\exp\left[-\mu^{-1}\int_\eta^z\gamma(\tau)\,d\tau\right]d\eta\,,\quad \mu>0\,;$$

$$u(z,\mu)=u_{\mathrm{bl}}(d)\exp\left[\mu^{-1}\int_z^d\gamma(\tau)\,d\tau\right]$$

$$-\mu^{-1}\int_z^d\left[\alpha(\eta)\,u_{\mathrm{bl}}(\eta)+\beta(\eta)\int_{-1}^{1}\sigma(\eta,\mu,\mu_1)\,u(\eta,\mu_1)\,d\mu_1\right]\exp\left[\mu^{-1}\int_z^\eta\gamma(\tau)\,d\tau\right]d\eta\,,\quad \mu<0\,.$$

There is no difficulty in reducing these equations to a single second-kind inhomogeneous Fredholm equation

$$u(\boldsymbol{\omega})-\int_\Omega K(\boldsymbol{\omega},\boldsymbol{\omega}_1)\,u(\boldsymbol{\omega}_1)\,d\boldsymbol{\omega}_1=f_0(\boldsymbol{\omega})\,,\quad \boldsymbol{\omega}=(z,\mu)\in\Omega=[0,d]\times[-1,1]\,, \tag{4}$$

where

$$K(\boldsymbol{\omega},\boldsymbol{\omega}_1)=(1-\theta(-\mu))\,K_+(\boldsymbol{\omega},\boldsymbol{\omega}_1)+(1-\theta(\mu))\,K_-(\boldsymbol{\omega},\boldsymbol{\omega}_1)\,; \tag{5}$$

$$f_0(\boldsymbol{\omega})=(1-\theta(-\mu))\,f_+(\boldsymbol{\omega})+(1-\theta(\mu))\,f_-(\boldsymbol{\omega})\,; \tag{6}$$

$$K_+(\boldsymbol{\omega},\boldsymbol{\omega}_1)=\theta(z-z_1)\,p_+(\boldsymbol{\omega},z_1)\,\sigma(z_1,\mu,\mu_1)\,,\quad K_-(\boldsymbol{\omega},\boldsymbol{\omega}_1)=\theta(z_1-z)\,p_-(\boldsymbol{\omega},z_1)\,\sigma(z_1,\mu,\mu_1)\,; \tag{7}$$

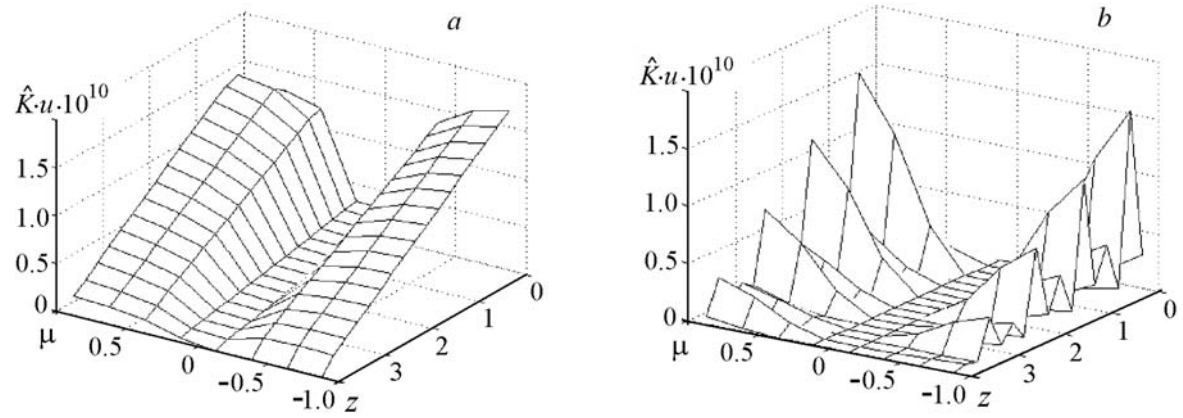

Fig. 7. Action of integral operator (4) on the linear function: a) accurate and b) with insufficient integration accuracy.

$$f_+(\boldsymbol{\omega}) = u_{\mathrm{bl}}(0)\, p(\mu, 0, z) + \mu^{-1} \int_0^z \alpha(z_1)\, u_{\mathrm{bl}}(z_1)\, p(\mu, z_1, z)\, dz_1 ;$$

$$f_-(\boldsymbol{\omega}) = u_{\mathrm{bl}}(d)\, p(-\mu, z, d) - \mu^{-1} \int_z^d \alpha(z_1)\, u_{\mathrm{bl}}(z_1)\, p(-\mu, z, z_1)\, dz_1 ; \tag{8}$$

$$p_+(\boldsymbol{\omega}, z_1) = \mu^{-1}\beta(z_1)\, p(\mu, z_1, z), \quad p_-(\boldsymbol{\omega}, z_1) = -\mu^{-1}\beta(z_1)\, p(-\mu, z, z_1) ; \tag{9}$$

$$p(\mu, a, b) = \exp\left[-\mu^{-1} \int_a^b \gamma(\tau)\, d\tau\right], \quad \theta(x) = \begin{cases} 1, & x \geq 0 ; \\ 0, & x < 0 . \end{cases} \tag{10}$$

Basic problems in its numerical solution arise primarily in the vicinity of eigensolutions of a homogeneous equation where the conditions of existence and uniqueness of the solution can be violated. However, such problems are physically little understood for the considered processes. Difficulties are also encountered when the kernel of an equation or its source lose smoothness or are fast-changing. In this case, for numerical integration to be adequate, use should be made of fine grids that appreciably increase the volume of calculations. The considered materials very frequently exhibit marked local nonuniformity and anisotropy of properties. Their effect on the numerical solution of Eq. (1) is direct and significant. In Eq. (4) it is mediated by the presence of integrals in both function p (10) and source (6). And though the exponent of the function p is not positive on the carriers of the kernel and source of Eq. (4), this function can enhance fluctuations of the attenuation coefficient, especially at small absolute values of μ.

On rough grids, the behavior of such a source, a kernel, and especially an integral operator of Eq. (4) can be distorted quite significantly, primarily for intensely scattering media. In practice, kinetic problems frequently have to be solved on relatively rough grids. If no special measures are taken to limit errors, the properties of the problem operators can be drastically distorted (Fig. 7).

The considered problem also involves serious difficulties linked with a possible significant optical layer thickness. The use of either optical coordinates or special scales, which extend the region of solution and thus smooth possible fluctuations of the equation components, does not solve the problem of the accumulated integration errors. However, they increase the volume of calculations. Furthermore, optical properties of the layer can also have a marked effect on the convergence of the method.

Discussed below are the method of numerical integration and the way of determining its accuracy that provides an adequate approximation of problem (4)–(10) as do the techniques allowing a decrease in requirements to the integration accuracy.

From the viewpoint of the above problems, extreme methods for which efficient tools of regularizing the solutions of unstationary problems have been developed, are affective. As a rule, in order to suppress errors, the functional of the solved extreme problems is completed with additional components, which changes the original functional [11, 12]. Yet, the techniques allowing one to avoid such complications are known [13].

Assume that $u \in U(\Omega)$ and $f_0 \in F(\Omega)$, where U and F are certain Hilbert spaces ($L_2(\Omega)$ is generally regarded as U and F). We introduce the operator

$$\hat{A} \cdot u(\boldsymbol{\omega}) = \int_{\Omega} (\delta(\boldsymbol{\omega}_1 - \boldsymbol{\omega}) - K(\boldsymbol{\omega}, \boldsymbol{\omega}_1)) u(\boldsymbol{\omega}_1) d\boldsymbol{\omega}_1, \quad \hat{A} : U \to F, \tag{11}$$

acting from U to F, and seek to minimize the residual functional $J(u) = \frac{1}{2}\|\hat{A} \cdot u - f_0\|_F^2$ of Eq. (4), $\hat{A} \cdot u = f_0$, in which the norm is matched to the scalar product determined on F. Following [13], for this we initially determine the gradient of the functional $J'(u)$ (the Frechet derivative). Since the operator $\hat{A}$ is linear, we have $J'(u) = \hat{A}^* \cdot (\hat{A} \cdot u - f_0)$. The conjugate operator $\hat{A}^* : F \to U$ is defined as usually by the bilinear identity $(\hat{A}u, f)_F = (u, \hat{A}^* f)_U$, $u \in U$, $f \in F$. Then, with allowance for expression (11), for U, $F = L_2$ we obtain

$$\hat{A}^* \cdot f(\boldsymbol{\omega}) = \int_{\Omega} (\delta(\boldsymbol{\omega}_1 - \boldsymbol{\omega}) - K(\boldsymbol{\omega}_1, \boldsymbol{\omega})) f(\boldsymbol{\omega}_1) d\boldsymbol{\omega}_1, \tag{12}$$

i.e. the conjugation of the operator $\hat{A}$ on $L_2(\Omega)$ reduces to the transposition of the kernel $K(\boldsymbol{\omega}, \boldsymbol{\omega}_1)$ of integral equation (4). With account for the deep analogy between Eq. (4) and linear algebraic systems, which follows from the Fredholm theory, this result is expected and quite understandable.

The gradient of the functional $J'(u)$ corresponding to expressions (11) and (12) is of the form

$$J'(u(\boldsymbol{\omega})) = u(\boldsymbol{\omega}) - f_0(\boldsymbol{\omega}) + \int_{\Omega} K(\boldsymbol{\omega}_1, \boldsymbol{\omega}) f_0(\boldsymbol{\omega}_1) d\boldsymbol{\omega}_1$$

$$- \int_{\Omega} [K(\boldsymbol{\omega}, \boldsymbol{\omega}_1) + K(\boldsymbol{\omega}_1, \boldsymbol{\omega})] u(\boldsymbol{\omega}_1) d\boldsymbol{\omega}_1 + \int_{\Omega} K(\boldsymbol{\omega}_1, \boldsymbol{\omega}) \int_{\Omega} K(\boldsymbol{\omega}_1, \boldsymbol{\omega}_2) u(\boldsymbol{\omega}_2) d\boldsymbol{\omega}_2 d\boldsymbol{\omega}_1 . \tag{13}$$

The residual functional can be minimized using the known conjugate-gradient method [11, 13, 14] studied in detail in [13]:

$$u_{n+1} = u_n - q_n \zeta_n, \quad \zeta_n = J'(u_n) + r_n \zeta_{n-1}, \quad n = 0, 1, 2, \ldots ;$$

$$q_n = \frac{(J'(u_n), \zeta_n)_U}{\|\hat{A}\zeta_n\|_F^2}, \quad r_n = \frac{\|J'(u_n)\|_U^2}{\|J'(u_{n-1})\|_U^2}, \quad r_0 = 0 . \tag{14}$$

Iteration sequence (14) has the properties of a monotonic superlinear convergence and a monotonic decrease of the residual on the accurate initial data $\{\hat{A}, f_0\}$. The grid approximation of the source f_0 and the operators $\hat{A}$ and $\hat{A}^*$ is one of the sources of inaccuracy of the data. Therefore, with an increase in the number of iterations and with the accumulation of computational errors the obtained approximations can noticeably differ from the exact solution. This necessitates a constant control over the residual of the solved equations.

An insufficiently accurate approximation of the problem operators can give rise to strong instabilities in the numerical solution. This is seen from the example presented in Fig. 7. However, the requirements for accuracy of the

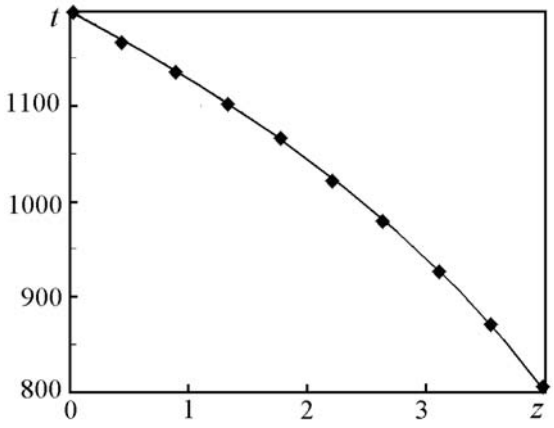

Fig. 8. Temperature profile. t, ^{o}C.

approximation of operators can be significantly decreased by imposing additional restrictions on the solution smoothness without changing the problem functional [13].

We will seek the solution $v(\boldsymbol{\omega}) \in V \subset U$, where V is the Hilbert space with a norm stronger than in U. This means that from convergence in the norm V should follow convergence in the norm U, but the reverse can be wrong. For example, instead of the solution from $U = L_2(\Omega)$ we will seek the solution from $V = W_2^1[0, d] \times L_2[-1, 1]$ with the scalar product $(u, v)_V = (u, v)_{L_2} + \tilde{\rho}\left(\frac{\partial u}{\partial z}, \frac{\partial v}{\partial z}\right)_{L_2}$ and the matched norm. Following [13], we introduce the operator $\hat{I}$ of enclosing the space V in the space U, which is the unit operator on $V \subset U$. The operator analog $Au = f_0$ of Eq. (4) is then replaced by the equation $\hat{A}\cdot\hat{I}v = f_0$, $u = \hat{I}v \equiv v$, and iteration sequence (14) assumes in U the following form:

$$u_{n+1} = u_n - q_n\zeta_n\,, \quad \zeta_n = \hat{I}^* J'(u_n) + r_n\zeta_{n-1}\,, \quad n = 0, 1, 2, \ldots\,;$$

$$q_n = \frac{(\hat{I}^* J'(u_n), \zeta_n)_V}{\|\hat{A}\zeta_n\|_F^2}\,, \quad r_n = \frac{\|\hat{I}^* J'(u_n)\|_V^2}{\|\hat{I}^* J'(u_{n-1})\|_V^2}\,, \quad r_0 = 0\,. \tag{15}$$

Here, $\hat{I}^* : U \to V$ is a nonidentical operator conjugate to $\hat{I}$. It plays the role of a stabilizing operator in U. For it, as can be easily shown, the following relations take place:

$$\hat{I}^* u = \frac{1}{\sqrt{\tilde{\rho}}}\left[a\cosh\left(\frac{z}{\sqrt{\tilde{\rho}}}\right) - \int_0^z \sinh\left(\frac{z-\eta}{\sqrt{\tilde{\rho}}}\right) u(\eta)\, d\eta\right], \quad a = \sinh^{-1}\left(\frac{d}{\sqrt{\tilde{\rho}}}\right)\int_0^d \cosh\left(\frac{d-\eta}{\sqrt{\tilde{\rho}}}\right) u(\eta)\, d\eta\,; \tag{16}$$

$$\frac{\partial}{\partial z}\hat{I}^* u = \frac{1}{\tilde{\rho}}\left[a\sinh\left(\frac{z}{\sqrt{\tilde{\rho}}}\right) - \int_0^z \cosh\left(\frac{z-\eta}{\sqrt{\tilde{\rho}}}\right) u(\eta)\, d\eta\right]. \tag{17}$$

Since integral equation (11) is not altered by the performed transformations, its residual functional is not changed either, which is significant. The parameter $\tilde{\rho}$, which determines the metric in V, is specified from considerations of optimizing the method operation and is selected proceeding from results of the computational experiment.

An evident case where an analytical solution of Eq. (4) can be obtained is the case of a nonscattering medium β, $\sigma \equiv 0$. Here, directly from the integral equations of radiation transfer it follows that

$$u(z, \mu) = u_{bl}(0)\exp\left[-\mu^{-1}\int_0^z \alpha(\tau)\, d\tau\right] + \mu^{-1}\int_0^z \alpha(\eta)\, u_{bl}(\eta)\exp\left[-\mu^{-1}\int_\eta^z \alpha(\tau)\, d\tau\right] d\eta\,, \quad \mu > 0\,; \tag{18}$$

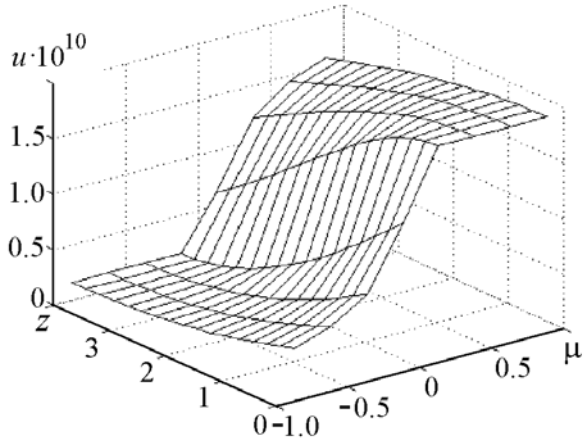

Fig. 9. Exact solutions (18) and (19).

$$u(z, \mu) = u_{\text{bl}}(d) \exp\left[\mu^{-1} \int_z^d \alpha(\tau)\, d\tau\right] - \mu^{-1} \int_z^d \alpha(\eta)\, u_{\text{bl}}(\eta) \exp\left[\mu^{-1} \int_z^\eta \alpha(\tau)\, d\tau\right] d\eta\,, \quad \mu < 0\,. \tag{19}$$

The form of functions (18) and (19) for a layer $d = 4$ of a homogeneous medium $\alpha = \gamma = 0.1$, whose temperature profile is given in Fig. 8, is shown in Fig. 9. Figures 10 and 11 present some results of relevant calculations by the above method with $\tilde{\rho} = 1$ and the Planck initial approximation. Use was made of a uniform 17×8 grid (z, μ), which is rather rough, and the Romberg integration method in which the order of the dominant term of error k_{R} on the integration step was a preset parameter. The presented results correspond to $k_R = 3$. The calculated radiation intensity is visually indistinguishable from the exact solution and therefore not shown additionally.

Figure 10 depicts the iteration-number dependence of residuals (a maximum of the modulus of the difference between the left- and right-hand sides) calculated for Eqs. (1) and (4). A similar dependence of the residual functional of the integral equation is shown in Fig. 11.

A fairly rapid convergence of the method in both residuals should be noted. The first steps of the method appreciably change the intensity. At this step of the solution the residual of the equations can even increase, especially if the initial approximation is sufficiently accurate. At these moments the initial distribution radically change. An additional artificial decrease in the depth of the sink q in these iterations only retards the beginning of this process. It should also be noted that with such, relatively low, accuracy of the integration on a fairly rough grid the convergence of iterations without stabilizing transformations (15) and (16) would have been lost.

Previously it has already been pointed out that insufficient integration accuracy can very markedly change the problem operators. Therefore, in analyzing the adequacy of the method it is important to compare calculated and analytical results of the effect of the problem operators on any simple distributions. For example, the action of the integral operator $\hat{K}$ of Eq. (4) on an isotropic radiation distribution gives

$$\hat{K} \cdot u(z) = \mu^{-1} \left[(1 - \theta(-\mu)) \int_0^z u(z_1)\, \beta(z_1)\, p(\mu, z_1, z)\, dz_1 - (1 - \theta(\mu)) \int_0^z u(z_1)\, \beta(z_1)\, p(-\mu, z, z_1)\, dz_1 \right].$$

In the case of the linear distribution, $u(z) = az + b$ in an optically homogeneous medium (β, γ = const). Herefrom follows this simple result:

$$\hat{K} \cdot (az + b) = \frac{\beta}{\gamma} \left\{ \left[\frac{\mu}{\gamma} - g(\mu) \right) a - b \right] \exp\left[\frac{\gamma (g(\mu) - z)}{\mu} \right] + a \left(z - \frac{\mu}{\gamma} \right) + b \right\}, \quad g(\mu) = \begin{cases} 0\,, & \mu > 0\,; \\ d\,, & \mu < 0\,, \end{cases} \tag{20}$$

which can be used for clarifying which integration accuracy is acceptable for the layer of the considered optical thickness. The results on Fig. 7 pertain exactly to the considered case where $d = 4$ and $\gamma = 6$. An adequate behavior of

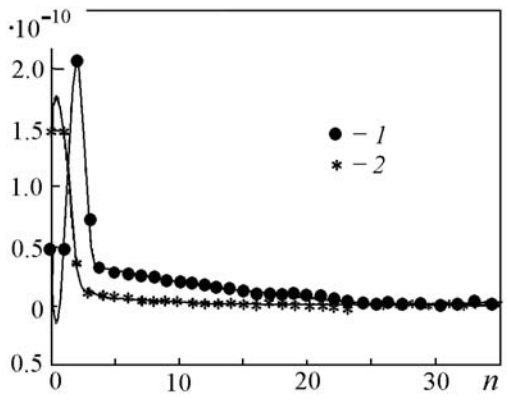

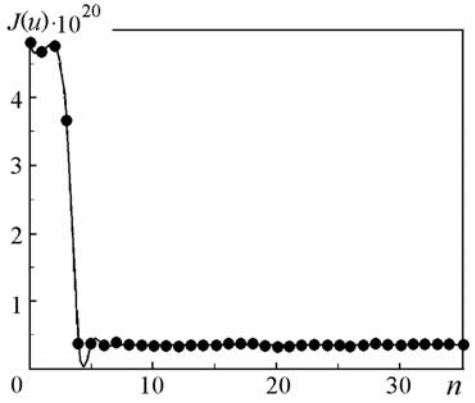

Fig. 10. Dependence of residuals (over the vertical) on the iteration number n: 1) Eq. (1) and 2) Eqs. (4).

Fig. 11. Dependence of the residual functional $J(u)$ on the iteration number n.

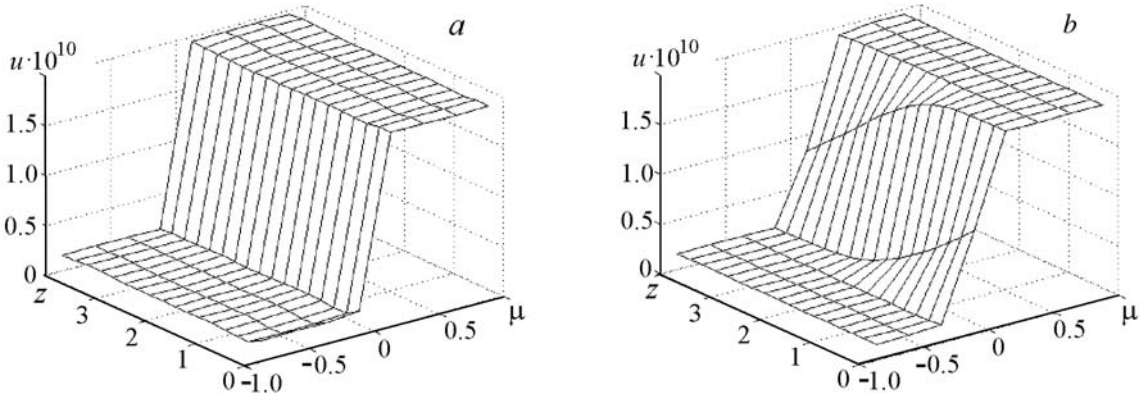

Fig. 12. Comparison of results calculated using the extreme method (a) and the time-dependent technique (b).

the expression $K\cdot(az + b)$ calculated on a rough 17 × 8 grid (z, μ) by a direct computation of the integral in Eqs. (4) is observed only for $k_R \geq 5$, since in the considered case the layer is optically fairly thick. The function in Fig. 7b corresponds to $k_R = 3$. At $k_R = 6$, the calculated action of the integral operator becomes undistinguishable from exact expression (20). However, these high requirements for accuracy practically preclude the use of the gradient method, since the time expenditure for calculating gradient (13), which contains a 4-fold integral, becomes exceedingly large. Practical work with the "step accessibility" method suggested on computers is possible if computations of *manifold* integrals are adequate when $k_R \leq 3$. An increase in the grid dimensions, especially along z, decreases requirements as to the integration accuracy. However, this problem should be solved in advance separately in each specific case. As seen, the method of functional optimization imposes high requirements on the integration accuracy. Therefore, its use for optically thick layers necessitates extensive computations, as is the case with any highly accurate method. Of course this circumstance limits the opportunities for its application. At the same time, the presented method is devoid of numerical diffusion and has a fairly reliable tool for controlling accuracy.

In Fig. 12, comparison is made of the results of solving the problem for a thin layer of an optically homogeneous weakly absorbing medium with nearly isotropic scattering, which were obtained by the method of the functional optimization described above (Fig. 12a) and in establishing the solution of the corresponding nonstationarity problem by an explicit method with three-step factorization (Fig. 12b). The following values were used in calculations: d = 0.04, $\alpha = 10^{-9}$, $\beta = \gamma = 0.1$, $\sigma \approx 0.5$, and k_R = 2–3. The extreme method leads to a solution practically having discontinuity at $\mu = 0$, while the time-dependent technique is characterized by significant numerical diffusion. The residual values for the extreme method are appreciably smaller than for the splitting method.

Since the time-dependent technique is simpler, it is less costly in time and practically indifferent to the initial approximation. Thus, this and similar methods can aid in obtaining numerical solutions that will be a good initial approximation for the proposed highly accurate extreme method. Probably exactly such combination of relatively rough but simple grid methods and a more accurate extreme method is optimal.

Conclusions. An efficient complex of software and experimental tools is developed, which allows determining and predicting thermal physical and optical properties of many promising materials with high accuracy. The proposed approach is based on thermal, rather than optical, experiments which generally require a complex and costly equipment. Many elements of the complex are independent efficient tools and can be applied to solving the problems of the investigation and development in various areas of science and engineering.

The work was carried out with support from ESTEC/ESA and EADS (the leading manufacturer Astrium GmBH), grant No. 3871 of the International Scientific and Engineering Center. The proposed mathematical models of materials are based on their experimental study and analysis of properties performed with direct participation of Doctor of Engineering A. V. Nenarokomov and S. A. Budnik (Moscow Aviation Institute).

NOTATION

A, effective coefficient of energy accommodation in the interaction of gas molecules with the material base; $a_{1,2}$, anisotropy indices in the coordinate directions orthogonal to heat transfer; $\hat{A}$ and $\hat{A}^*$, operator (11) and operator (12) conjugate to it; b, average pore size; d, dimensionless thickness of the layer of the radiation transfer problem; $\langle d \rangle$, average fiber diameter; $d_{b,k}$, center of the kth interval of the histogram of the foam material nodes; d_k, center of the kth interval of the histogram of diameters of the foam material bridges; $d_{n,m}$, center of the mth material of the histogram of diameters of n-type fibers ((n, m) fibers); F, f, space of free terms of the integral equation and its element; $f_0 \in F$, free term of integral equation (4); $f_\pm$, auxiliary functions (8); $g(\mu)$, auxiliary function (20); $\hat{I}$, operator of enclosing the space V in U; J, J', residual functional and its gradient (the Frechet derivative); K, kernel (5) of integral equation (4); $\hat{K}$, integral operator of Eq. (4); $K_\pm$, auxiliary functions (7); k_R, order of the error of numerical integration by the Romberg method; $l_{n,k}$, center of the kth interval of the foam material histogram for lengths of the bridges with diameters from the nth interval ((n, k) bridges); $l_{n,m,k}$, center of the kth interval of the histogram of length of (n, m)-fibers; N_b, number of intervals on the histogram the node diameters of a foam material; N_d, number of intervals on the histogram of fiber diameters; N_{len}, number of intervals on the histogram of fiber lengths and bridges; N_t, amount of substances of which the material fibers are manufactured; p, p_0, actual and normal pressures; $p_\pm$ and p, auxiliary functions (9) and (10) of the optical problem; P_k, probability of observing k-type fibers; $P_{n,m}$, conventional probability of observing fibers and bridges of the (n, m)-type; $P_{n,m,k}$, fraction of (n, m)-type fibers with a length from the kth interval of the histogram; Pr, Prandtl number; q and r, variables of conjugate-gradient method (14); U and u, space of solutions of the radiation transfer problem and its element; u_{bl} radiation intensity of a blackbody; V and v, Sobolev space of stabilized solutions and its element; t and T, temperature, degrees Celsius and Kelvin, respectively; x, geometric parameters of representative elements: the element dimension in the direction of heat transfer for fibrous materials and the coefficient of cutting off of bridges for foam materials; z, dimensionless Cartesian coordinate transverse to the layer; z_1, integration variable; α, β, $\gamma = \alpha + \beta$, coefficients of absorption, scattering, and attenuation; $\tilde{\gamma}$, specific heat ratio of gas in pores at normal pressure; $\delta(x)$, Dirac function; ζ, variable of conjugate-gradient method (14); η, integration variable; $\theta(x)$, Heaviside function; ϑ, polar angle; Λ_0, free path of gas in pores at normal pressure; λ_c, conductive thermal conductivity of a porous material; λ_{eff}, total (effective) thermal conductivity of a porous material; λ_{g0}, thermal conductivity of gas in pores at normal pressure; λ_p, thermal conductivity of the effective gas with allowance for porosity; λ_r, radiative thermal conductivity of a porous material; $\mu = \cos\vartheta$; μ_1, integration variable; ρ, effective mass density of a highly porous material; $\tilde{\rho}$, metric coefficient of the Sobolev space V; ρ_0, density of the substance of which the foam-material base is made; ρ_k, density of the k-type material; σ, indicatrix averaged over the azimuths of incident and scattered radiation; τ, integration variable; φ, azimuthal angle; Ω, region of determining the solution of radiation problem (4)–(6); $\mathbf{\Omega}$, unit vector of the direction; $\boldsymbol{\omega} = (z, \mu)$, vector of arguments; $\boldsymbol{\omega}_{1,2}$, vector integration variables. Subscripts: b, ball; bl, radiation of a blackbody; d, diameter; len, length; eff, effective (total); g, gas; c, conductive; t, type (material); p, porosity; r, radiative.

REFERENCES

1. O. M. Alifanov, *Inverse Heat Transfer Problems*, Springer Verlag, Berlin (1994).
2. O. M. Alifanov, S. A. Budnik, V. V. Mikhailov, and A. V. Nenarokomov, An experimental-computational complex for studying thermophysical properties of thermal-engineering materials, *Tepl. Prots. Tekh.*, **1**, No. 2, 49–60 (2009).
3. G. N. Dul'nev and Yu. P. Zarichnyak, *Thermal Conductivity of Mixtures and Composite Materials* [in Russian], Énergiya, Leningrad (1974).
4. O. M. Alifanov and N. A. Bojkov, Les Methodes des Previsions in Formatiquers des Materaux Composities de Haute Porosite et de L' and Tanalise des Systems de la Protection Thermique a leur Basc, in: *Proc. Conf. on Spacecraft Structures, Materials and Mechanical Testing*, Noordwijk, The Netherlands, 27–29 March, 1996 (ESA SP-386, June 1996).
5. O. M. Alifanov and V. V. Cherepanov, Mathematical simulation of highly porous fibrous materials and determination of their physical properties, *Teplofiz. Vys. Temp.*, **47**, No. 3, 463–472 (2009).
6. Ya. B. Zel'dovich and Yu. P. Raizer, *Physics of Shock Waves and High-Temperature Hydrodynamic Phenomena* [in Russian], Nauka, Moscow (1966).
7. C. F. Bohren and D. R. Huffman, *Absorption and Scattering of Light by Small Particles* [Russian translation] Mir, Moscow (1986).
8. L. A. Dombrovskii, Calculation of spectral radiative characteristics of quartz fibrous thermal insulation in the infrared region, *Teplofiz. Vys. Temp.*, **32**, No. 2, 209–215 (1994).
9. V. K. Leko and O. V. Mazurin, *The Properties of Quartz Glass* [in Russian], Nauka, Leningrad (1985).
10. M. N. Ozisik, *Combined Heat Transfer* [in Russian], Mir, Moscow (1976).
11. N. N. Kalitkin, *Numerical Methods* [in Russian], Mir, Moscow (1978).
12. E. M. Mamedov and S. A. Rukolaine, Numerical solution of the problems of radiative heat transfer in irregularly shaped regions with specular (Fresnel) boundaries. Axisymmetrical case, *Mat. Modelir.*, **16**, No. 10, 15–28 (2004).
13. O. M. Alifanov, E. A. Artyukhin, and S. V. Rumyantsev, *Extreme Methods of Solving Ill-Posed Problems* [in Russian], Nauka, Moscow (1988).
14. V. G. Karmanov, *Mathematical Programming* [in Russian], Nauka, Moscow (1980).